

Identifying Swing Dynamic Coherency by Koopman Mode Analysis

Zahra Jlassi^{#1}, Khadija Ben Kilani^{#2}, Mohamed Elleuch^{#3}, Lamine Mili^{*4}

[#] ENIT-L.S.E-LR11ES15, University of Tunis EL Manar
Tunis le Belvédère, Tunisia

¹jlassi.zahra@hotmail.fr

²khadijakilani@yahoo.fr

³mohamed.elleuch@enit.utm.tn

^{*} Electrical Engineering Department, Virginia Polytech. Inst. & State University
Blacksburg, VA, USA

⁴lmili@vt.edu

Abstract— This paper provides a new technique to identify coherent machines groups of electrical power systems swinging together in frequency and phase. Modal analysis of swing dynamics under large disturbances in multi-machine networks is performed based on a mathematical technique named Nonlinear Koopman Mode Analysis. The study is conducted on two tested networks: the Kundur 2-area 4-machines power system and the IEEE 9-bus 4-machines power system. A comparison of the Discrete Fourier Transform analysis is carried out with the nonlinear Koopman mode analysis in terms of frequencies and coherency identification. This comparison reveals that the Koopman modes extract spatial single-frequency oscillations and may identify coherent swings dynamics.

Keywords— Electrical Power Systems, Nonlinear Oscillations, Koopman Mode Analysis, Transient stability, Coherency Identification.

I. INTRODUCTION

Electrical power grid is the most complex dynamical man-made system there is. It experiences various types of oscillations [1] [2] which are excited by disturbances. As examples of oscillation modes, we distinguish the inter-area modes and the local generator modes [3].

Coherency identification is one of the essential applications of modes identification. For transient stability analysis, a group of synchronous generators is coherent if these generators swing together in frequency and phase. There are many objectives for identifying coherency, such as the reduced-order models development, the assessment of on-line dynamic security and the analysis of electrical power system instabilities [4]. Many researchers have developed methods for the identification of coherency. In [5] the author used the time domain simulation of the linearized power system models for the analysis of coherent generators subject to disturbances. The authors in [6] [7] applied time-scale separation used to power system models for singular perturbation studies. In [7]–[10] the authors developed grouping algorithms by using slow coherency to identify coherent generators groups in power

system. In [11]–[13], the authors studied the coherency by the use of linear and decentralized systems theories such as the weak coupling idea. The authors in [14] [15] used the energy function in order to identify coherent generators.

Large-scale electrical networks have various types of nonlinearities. The modeling and the analyzing of their dynamics are very difficult. One more traditional mode notion usually carried out which is developed in electrical power system stability analysis was based on the small-signal dynamics which investigate linearized equations around equilibrium [16] [17]. However, large disturbance will pull network operating point far away from the stable equilibrium point. Nonlinear interactions will be disregarded from the analysis. Hence, linear approximation may be invalid. Therefore, developing new technique for identifying modes without relying on linearization is a recurring need. Recently, a mathematical technique of nonlinear modal decomposition has gained increased attention as a new technique applied to power system called Koopman Mode Analysis (KMA) [16] [17] [24]–[27]. This theory is based on the linear and infinite-dimensional Koopman operator [18] [19]–[23]. The KMA is applied on snapshot measurements or simulated data following disturbances. It extracts significant spatio-temporal characteristics.

This paper deals with the application of the KMA to identify coherent machines groups of electrical networks swinging together in frequency and phase. This identification method is based on the analysis of swing dynamics following large disturbances. The study is conducted on two tested networks: the Kundur two area 4-machines power system and the IEEE 9-bus 4-machines power system. A comparison of the Discrete Fourier Transform (DFT) analysis is carried out with the nonlinear KMA in terms of frequencies and coherency identification. This comparison reveals that the Koopman modes extract spatial single-frequency oscillations and may identify coherent swings dynamics, whereas the Discrete Fourier Transform may not identify generators coherency because it does not consider phase information.

II. THE KOOPMAN MODE ANALYSIS

A. Koopman Mode Theory

Koopman pioneered the linear transformations used on Hilbert space with the aim to analyse Hamiltonian systems by introducing the Koopman operator and its spectrum study [28]-[30]. The KMA is a mathematical technique of modal decomposition for nonlinear dynamics based on the Koopman operator spectral analysis which is defined for nonlinear or linear system. [20] [21] Even if the dynamic observed data are finite dimensional, this operator is infinite dimensional and it doesn't rely on any linearization of dynamics.

The following development is based on [21]. Consider the dynamics which are described by discrete time, a nonlinear difference equation manifold M:

$$x_{k+1} = f(x_k) \quad (1)$$

Where f is a nonlinear map from M to itself. The Koopman operator acts on $g: M \rightarrow \mathbb{R}$ an observable scalar function defined as follow:

$$U g(x) = g(f(x)) \quad (2)$$

The j -th Koopman eigenvalues $\lambda_j \in \mathbb{C}$ and eigenfunctions $\varphi_j: M \rightarrow \mathbb{C}$ are defined as:

$$U \varphi_j(x) = \lambda_j \varphi_j(x) \quad \text{For } j=1, 2 \dots \quad (3)$$

Let $g: M \rightarrow \mathbb{R}^p$ be a vector-valued observable. If each g_i of the components in g lies within the span of eigenfunctions φ_j , then the time-evolution of the observable $g(x_k)$ from $g(x_0)$ is expanded as follows:

$$g(x_k) = \sum_{j=1}^{\infty} U^k \varphi_j(x_0) v_j = \sum_{j=1}^{\infty} \lambda_j^k \varphi_j(x_0) v_j \quad (4)$$

Where v_j corresponds to the j -th Koopman mode. It is the vector-valued coefficient of the decomposition. This decomposition is based on the properties of the point spectrum of U , and the analysis based on (4) is the Koopman Mode Analysis.

B. Koopman Mode Analysis Algorithm

The computation of Koopman modes algorithm is resumed in Fig. 1. The input data of this algorithm are:

- Sampled snapshot measurements or simulated data such as the rotors angles speeds of the network following a disturbance with a desired sampling frequency « f_s ».
- The observables data Matrix « X » as shown in Fig. 2 where the columns of this matrix are defined as the measurements and its lines define the time evolution of the observables at $t = t_k$ [23]-[27].
- The Number « N_b » of desired Koopman modes to be computed by KMA algorithm. Although the choice of this number is arbitrary, it depends on the needed application and objective.

The KMA algorithm steps are as follow [23]-[27]:

1. Compute the matrix « A » and « B » defined as :

$$A = X1 * (X1)^T \quad (5)$$

$$B = X1 * (g(x_n))^T \quad (6)$$

Where « $X1$ » is the observables data matrix without the last line « $g(x_n)$ ».

2. Compute the companion matrix « C » :

$$C = \begin{bmatrix} 0 & 0 & \dots & 0 & c_0 \\ 1 & 0 & \dots & 0 & c_1 \\ 0 & 1 & & 0 & c_2 \\ \vdots & & \ddots & & \vdots \\ 0 & 0 & \dots & 1 & c_{N-1} \end{bmatrix} \quad (7)$$

It is defined as the product of the computed matrix « B » and the Moore Penrose pseudoinverse of computed matrix « A »:

$$C = A^+ B \quad (8)$$

3. Compute the Koopman eigenvalues $\tilde{\lambda}_j$ defined as the eigenvalues of the computed companion matrix « C ».
4. Define the Vandermonde matrix « T »:

$$T = \begin{bmatrix} 1 & \tilde{\lambda}_1 & \tilde{\lambda}_1^2 & \dots & \tilde{\lambda}_1^{N-1} \\ 1 & \tilde{\lambda}_2 & \tilde{\lambda}_2^2 & \dots & \tilde{\lambda}_2^{N-1} \\ 1 & \tilde{\lambda}_3 & \tilde{\lambda}_3^2 & \dots & \tilde{\lambda}_3^{N-1} \\ \vdots & \vdots & \vdots & \ddots & \vdots \\ 1 & \tilde{\lambda}_N & \tilde{\lambda}_N^2 & \dots & \tilde{\lambda}_N^{N-1} \end{bmatrix} \quad (9)$$

5. Compute the Koopman eigenvectors \tilde{v}_j which refer to the Koopman modes corresponding to the observables. They are defined as the columns of the matrix « V » :

$$V = [g(x_0), \dots, g(x_{N-1})] T^{-1} \quad (10)$$

The KMA algorithm outputs are [12]-[16]:

- The j Koopman eigenvalues $\tilde{\lambda}_j$ and modes \tilde{v}_j .
- The Koopman modes frequencies f_{KM} which are defined as:

$$f_{KM} = (\arg \tilde{\lambda}_j * f_s) / 2\pi \quad (11)$$

Where f_s is the sampling frequency and $\arg \tilde{\lambda}_j$ are the Koopman modes arguments defined as:

$$\arg \tilde{\lambda}_j = \text{Im}(\ln(\tilde{\lambda}_j)) \quad (12)$$

- The Koopman modes growth rates « GR » which are defined as the complex modulus of the Koopman eigenvalues given by:

$$GR = \|\tilde{\lambda}_j\| \quad (13)$$

This parameter evaluates the sampled dynamics damping. Indeed, a GR smaller than unity stands for a positively damped oscillatory mode. But a GR equal or larger than unity determines a non-oscillatory dynamics of power grid [16]-[17] [24]-[27]. Therefore, largest growth rates of modes indicate its smallest damping ratios.

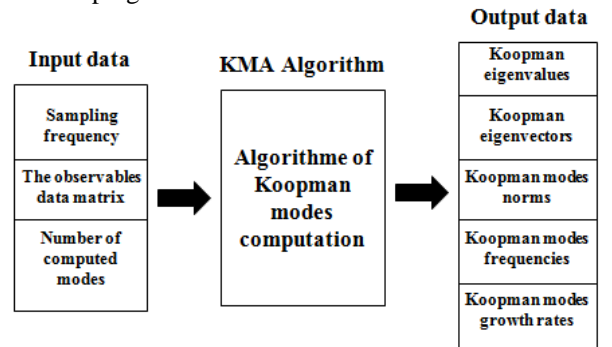


Fig. 1 KMA Algorithm

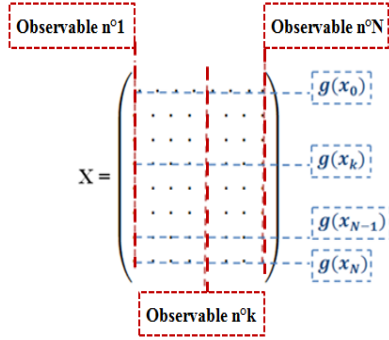


Fig. 2 Observables data Matrix

C. Coherency in Koopman modes

The notion of coherency in the context of Koopman modes is defined on [16]-[17] [24]-[25]. The study of this notion in power systems deals with oscillatory responses under disturbances. Hence, the case of an oscillatory Koopman mode which is characterised by an imaginary part of Koopman eigenvalue is addressed. For a given oscillatory Koopman mode v_j , called Koopman Mode j , with an eigenvalue $\lambda_j = r_j e^{i2\pi\nu j}$ and a complex conjugate eigenvalue $\lambda_j^c = r_j e^{-i2\pi\nu j}$, the corresponding modal dynamics $g^j(x_k)$ are defined by [24]-[25]:

$$g^j(x_k) = \lambda_j^k \varphi_j(x_0)v_j + (\lambda_j^c)^k \{\varphi_j(x_0)v_j\}^c \quad (14)$$

$$= 2r_j^k \begin{bmatrix} A_{j1} \cos(2\pi k\nu j + \alpha_{j1}) \\ \vdots \\ A_{jp} \cos(2\pi k\nu j + \alpha_{jp}) \end{bmatrix} \quad (15)$$

Where

$$A_{ji} = \sqrt{(\text{Re}[\varphi_j(x_0)v_j]_i)^2 + (\text{Im}[\varphi_j(x_0)v_j]_i)^2} \quad (15)$$

$$\tan \alpha_{ji} = \frac{\text{Im}[\varphi_j(x_0)v_j]_i}{\text{Re}[\varphi_j(x_0)v_j]_i} \quad (16)$$

The notation $\text{Re}[\varphi_j(x_0)v_j]_i$ determines the i -th component of vector $\text{Re}[\varphi_j(x_0)v_j]$ [24]-[25]. The real part of $\varphi_j(x_0)v_j$ stands for the initial amplitude of the modal dynamics. Its imaginary part is affected by their initial phase [24]-[25]. To identify coherent swing dynamics of synchronous generators in frequency and phase for a given Mode j , it is largely sufficient to check both the amplitude coefficients A_{ji} and the initial phases α_{ji} [24]-[25]. Indeed, a set of oscillatory components $I \subseteq [1... p]$ is defined as coherent group swinging together with respect to Mode j , if all $i \in I$ have the same amplitude coefficients and initial phases [24]-[25].

III. STUDY CASES

The KMA algorithm is applied to nonlinear swing dynamics in two study test power systems:

- The Kundur 2-area 4-machines power system given in Fig. 3. It contains two synchronous equivalent generators, a load and a capacitor in each area. Totally 3400 MWs of system generation capacity are installed in this study network.

Approximately 242 MW is exported from area 1 to area 2. Each test system generator is equipped with automatic regulators with the exception of one.

- The IEEE 9-bus 4-machines power system given in Fig. 4. It contains four synchronous generators equipped with automatic voltage and speed regulators. There are two generators equipped with Power System Stabilizer (PSS). Totally 46060 MWs of system generation capacity are installed in this study network. The simulation dynamics are performed using an open-source power system analysis toolbox (PSAT) of MATLAB [31].

The KMA is performed on sampled data of the generators angular speeds dynamics following three-phase short-circuit fault. The sampling frequency is 80Hz and the number of samples is 1600 for the two study test systems. The oscillation frequencies of obtained modes and the swing dynamic coherency identification are compared for both methods of analysis: the KMA and the Discrete Fourier Transform (DFT) of study dynamics.

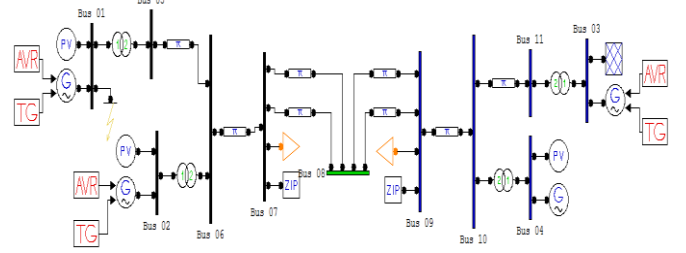


Fig. 3 Tested 2-area 4-machines power system modelled in PSAT

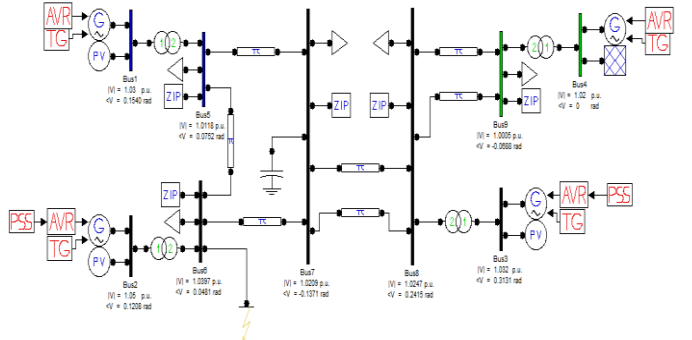


Fig. 4 Tested IEEE 9-bus 4-machines power system modelled in PSAT

IV. SIMULATION RESULTS

A. Simulation Settings

The studied disturbance is a three-phase short-circuit:

- For the case of Kundur 2-area 4-machines test system: the fault is applied at bus 1 at $t=1$ s and cleared at $t=1.09$ s. The simulation results are shown in Fig.5. We note that following this tested short circuit, generators 1 and 2 are swinging together in frequency and phase and the other generators 3 and 4 also show coherent swing excited by this applied disturbance. Note that this way of selecting coherent machines is heuristic by the check of their swing forms. These generators are called a coherent group.
- For the case of IEEE 9-bus 4-machines test system: the fault is applied at bus 6 at $t=1$ s and cleared at $t=1.15$ s. The

simulation results are shown in Fig.6. We note that following this tested short circuit, each generator has a different swing dynamic in frequency and phase compared to the other generators swing dynamics.

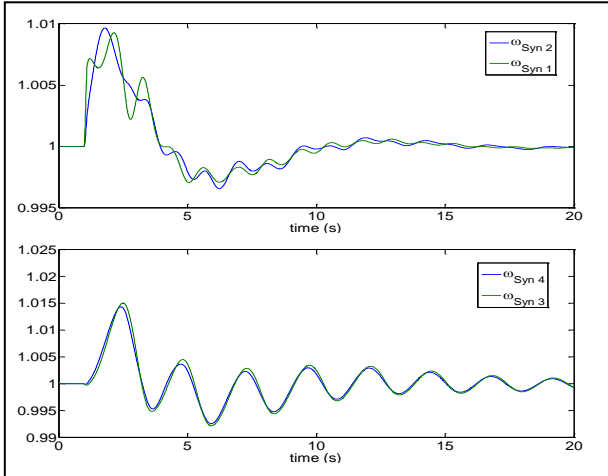


Fig. 5 Rotor angle speeds of generators following the tested three-phase fault for the tested 2-area 4-machines system

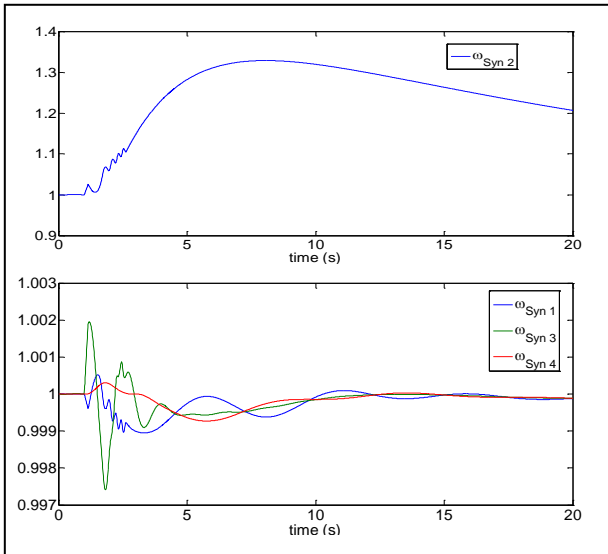


Fig. 6 Rotor angle speeds of generators following the tested three-phase fault for the tested 9-bus 4-machines system

B. Comparison of Results

1) *Frequencies identification:* For the two study test systems, the computed frequencies results of the KMA are compared with frequencies obtained by the DFT of study swing dynamics. The KMA detects full system details that are linear and nonlinear oscillatory modes. Note that evaluating the magnitudes of Koopman modes growth rates and norms is a condition to decide on the Koopman mode dominance. Table I provides frequencies results for the tested networks only of the three most dominant Koopman modes with largest GR and norm. Fig. 7, Fig. 8, Fig. 9 and Fig. 10 show the DFT of different time responses shown in Fig.5. Fig. 11 shows the DFT of generator 2 time response shown in Fig.6. The

application of the DFT to the other generators time response shown in Fig.6 illustrates any frequency peaks. The comparison between the KMA and the DFT frequencies results reveals that frequencies results of the three most dominant Koopman modes have the largest peaks obtained by the DFT.

TABLE I
FREQUENCIES RESULTS OF DOMINANT KOOPMAN MODES FOR THE TWO TESTED POWER SYSTEM

Tested 2-area 4-machines network	Tested 9-bus 4-machines network
0.41	0.054
0.11	0.10
0.15	0.15

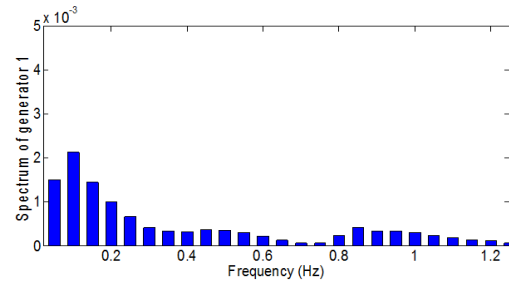


Fig. 7 DFT of time response shown in Fig.5 for generator 1

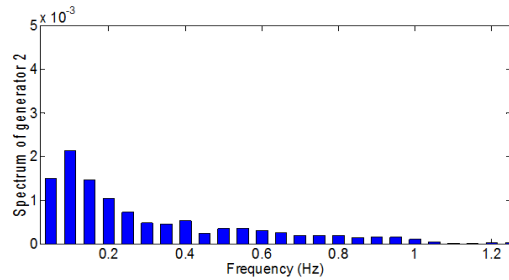


Fig. 8 DFT of time response shown in Fig.5 for generator 2

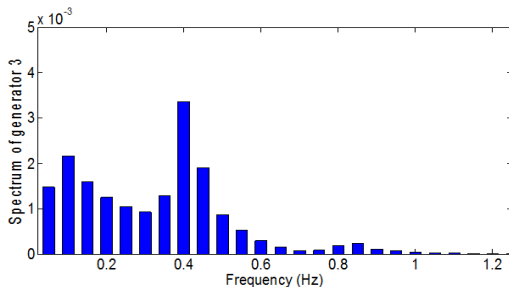


Fig. 9 DFT of time response shown in Fig.5 for generator 3

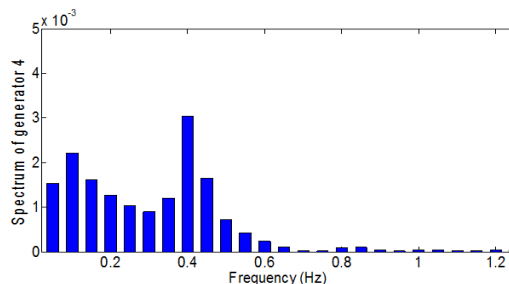


Fig. 10 DFT of time response shown in Fig.5 for generator 4

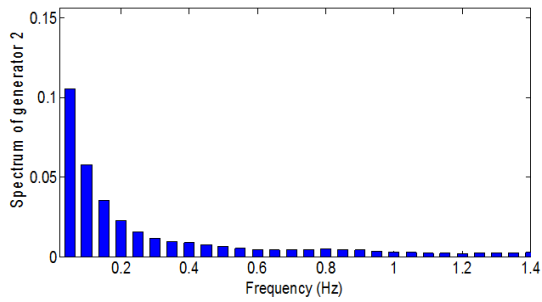


Fig. 11 DFT of time response shown in Fig.6 for generator 2

2) *Coherency identification*: Because the DFT doesn't consider phase information, we cannot conclude from the DFT results that a given machines swing coherently or not. However, the decomposition into Koopman modes makes the extraction of coherent generators possible in the coupled swing dynamics. In fact, for the case of tested 2-area 4-machines system, the dominant Koopman modes of frequencies 0.41 Hz and 0.11 Hz capture a coherent motion which is related to the two coherent machines groups: the group of generators 1 and 2 and the group of generators 3 and 4 as shown in Fig.12 and Fig.13. For the case of tested 9-bus 4-machines system, the generators show incoherent swings for the dominant Koopman modes of frequencies 0.054 Hz and 0.15 Hz as shown in Fig.14 and Fig.15.

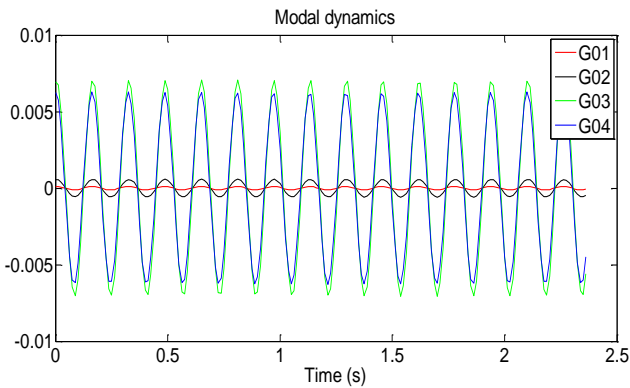


Fig. 12 Coherency in Koopman mode of frequency 0.41 Hz for tested 2-area 4-machines network

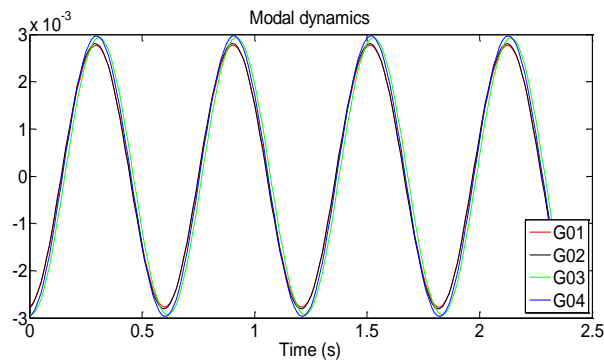


Fig. 13 Coherency in Koopman mode of frequency 0.11 Hz for tested 2-area 4-machines network

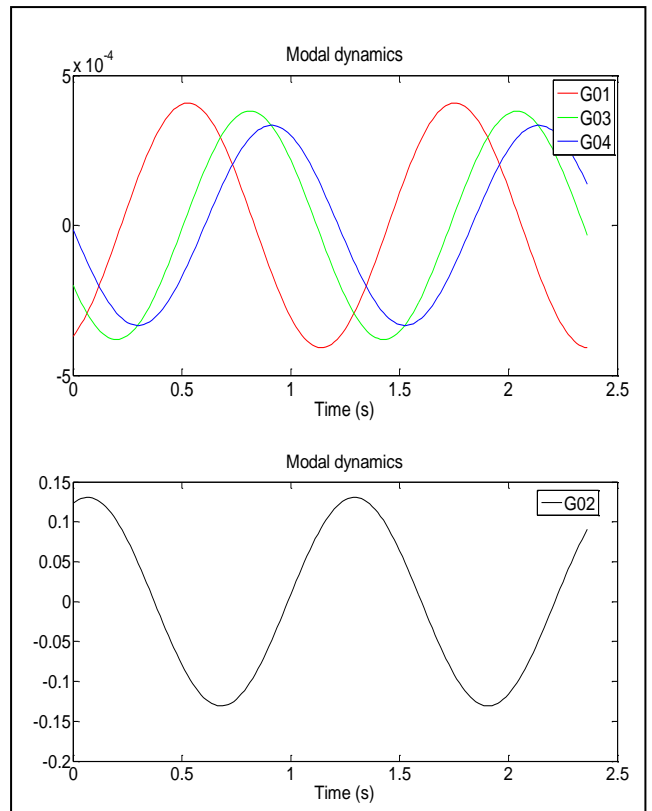


Fig. 14 Coherency in Koopman mode of frequency 0.054 Hz for tested 9-bus 4-machines network

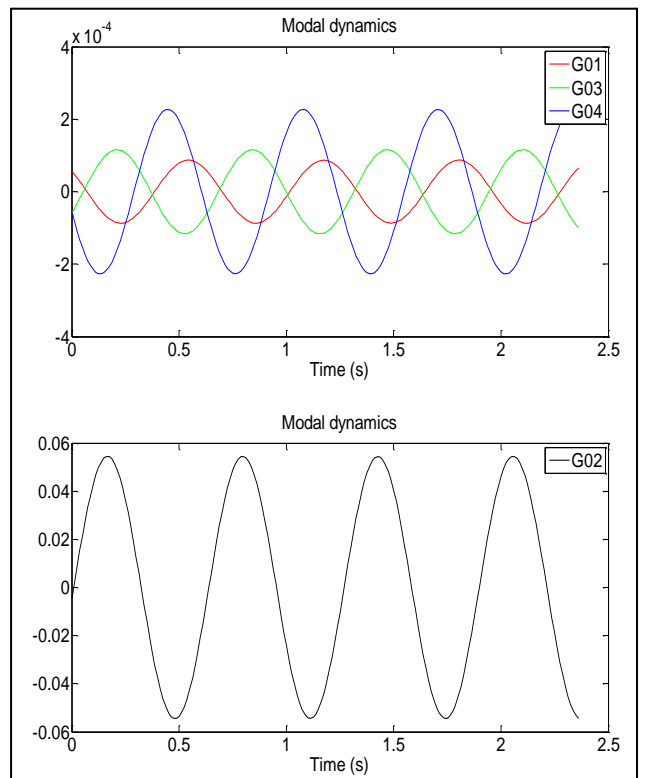


Fig. 15 Coherency in Koopman mode of frequency 0.15 Hz for tested 9-bus 4-machines network

V. CONCLUSIONS

This paper addressed the issue of characterizing global behavior of highly nonlinear spatiotemporal dynamics by their decomposing into Koopman modes. This recent technique of Koopman mode analysis is applied to short-term swing dynamics following large disturbances in two tested power systems: the Kundur 2-area 4-machines power system and the IEEE 9-bus 4-machines power system.

A comparison between the Koopman mode analysis and the Discrete Fourier Transform is performed in terms of frequencies and coherency identification. The comparison reveals that frequencies results of the most dominant Koopman modes have the largest peaks obtained by the DFT. We cannot conclude from the DFT results that a given machines swing coherently or not because the DFT doesn't consider phase information.

Our contributions in this paper are as follows: We show that Koopman mode analysis, a recently used technique in power systems analysis allows to:

- Identify spatial single-frequency modes embedded in nonlinear coupled swing dynamics.
- Identify coherent swings and machines.

These identifications are performed on dynamics finite-time data and don't require any direct check of spatiotemporal patterns.

REFERENCES

- [1] E. Barocio, Bikash C. Pal, Nina F. Thornhill, A.R. Messina, "A Dynamic Modes Decomposition Framework for Global Power System Oscillation Analysis," *IEEE Transactions on Power Systems*, vol. 30, no. 2, pp. 2012-2912, 2015.
- [2] E. H. Abed and P. P. Varaiya, "Nonlinear oscillations in power systems," *International Journal of Electrical Power & Energy Systems*, vol. 6, pp. 37-43, 1984.
- [3] M. Klein, G. Rogers, and P. Kundur, "A fundamental study of inter-area oscillations in power systems," *IEEE Transactions on Power Systems*, vol. 6, pp. 914-921, 1991.
- [4] Y. Susuki, I. Mezic, and T. Hikiyara, "Global swing instability of multimachine power systems," in *Proceedings of the 47th IEEE Conference on Decision and Control*, Cancun, Mexico, December 9-11 2008, pp.2487-2492.
- [5] R. Podmore, "Identification of coherent generators for dynamic equivalents," *IEEE Transactions on Power Apparatus and Systems*, vol. PAS- 97, no. 4, pp. 1344-1354, July/August 1978.
- [6] B. Avramovi'c, P. V. Kokotovic, J. R. Winkelman, and J. H. Chow, "Area decomposition for electromechanical models of power systems," *Automatica*, vol. 16, pp. 637-648, November 1980.
- [7] J. H. Chow, Ed., *Time-Scale Modeling of Dynamic Networks with Applications to Power Systems*, ser. Lecture Notes in Control and Information Sciences 46. Berlin Heidelberg: Springer-Verlag, 1982.
- [8] J. H. Chow, J. Cullum, and A. Willoughby, "A sparsity-based technique for identifying slow-coherent areas in large power systems," *IEEE Transactions on Power Apparatus and Systems*, vol. PAS-103, no. 3, pp. 463-473, March 1984.
- [9] S. B. Yusof, G. J. Rogers, and R. T. H. Alden, "Slow coherency based network partitioning including load buses," *IEEE Transactions on Power Systems*, vol. 8, no. 3, pp. 1375-1382, August 1993.
- [10] J. H. Chow, "New algorithms for slow coherency aggregation of large power systems," in *Systems and Control Theory for Power Systems*, J. H. Chow, P. V. Kokotovic, and R. J. Thomas, Eds. New York: Springer-Verlag, 1995, pp. 95-115.
- [11] S. Sastry and P. Varaiya, "Coherency for interconnected power systems," *IEEE Transactions on Automatic Control*, vol. AC-26, no. 1, pp. 218- 226, February 1981.
- [12] G. Troullinos and J. Dorsey, "Coherency and model reduction: State space point of view," *IEEE Transactions on Power Systems*, vol. 4, no. 3, pp. 988-995, August 1989.
- [13] R. Nath, S. S. Lamba, and K. S. Prakasa Rao, "Coherency based system decomposition into study and external areas using weak coupling," *IEEE Transactions on Power Apparatus and Systems*, vol. 104, no. 6, pp. 1443-1449, June 1985.
- [14] Y. Ohsawa and M. Hayashi, "Construction of power system transient stability equivalents using the Lyapunov function," *International Journal of Electronics*, vol. 50, no. 4, pp. 273-288, April 1981.
- [15] M. H. Haque and A. H. M. A. Rahim, "Identification of coherent generators using energy function," *IEE Proceedings, Part C*, vol. 137, no. 4, pp. 255-260, July 1990.
- [16] Fredrik Raak, "Investigation of Power Grid Islanding Based on Nonlinear Koopman Modes", Master of Science Thesis in Electric Power Systems, School of Electrical Engineering Royal Institute of Technology Stockholm, Sweden, September 2013.
- [17] Ahmad Anan Tbaileh, "Power System Coherency Identification Using Nonlinear Koopman Mode Analysis", Master of Science Thesis in Electrical and Computer Engineering, Faculty of Virginia Polytechnic Institute and State University, May 2014.
- [18] Kevin K Chen, Jonathan H Tu, and Clarence W Rowley. Variants of Dynamic Mode Decomposition: Boundary Condition, Koopman, and Fourier Analyses. *Journal of Nonlinear Science*, April 2012.
- [19] A. Ruhe, "Rational Krylov sequence methods for eigenvalue computation," *Linear Algebra Appl.*, 58:391-405, 1984.
- [20] I. Mezic, "Spectral properties of dynamical systems, model reduction and decompositions," *Nonlinear Dyn.*, vol. 41, pp. 309-325, August 2005.
- [21] C. W. Rowley, I. Mezic, S. Bagheri, P. Schlatter, and D. S. Henningson, "Spectral analysis of nonlinear flows," *Journal of Fluid Mechanics*, vol. 641, pp. 115-127, 2009.
- [22] B. Eisenhower, T. Maile, M. Fischer, and I. Mezic, "Decomposing building system data for model validation and analysis using the Koopman operator," in *Proceedings of the National IBPSAUSA Conference*, New York, USA, 2010.
- [23] M. Budisic, R. Mohr, and I. Mezic, "Applied Koopmanism," *Chaos: An Interdisciplinary Journal of Nonlinear Science*, vol. 22, no. 4, 2012.
- [24] Fredrik Raak, Y. Susuki, T. Hikiyara, "Data-Driven Partitioning of Power Networks via nonlinear Koopman Mode Analysis," *IEEE Transactions on Power Systems*, 2015.
- [25] Y. Susuki and I. Mezic, "Nonlinear Koopman modes and coherency identification of coupled swing dynamics," *IEEE Transactions on Power Systems*, vol. 26, no. 4, 2011.
- [26] Y. Susuki and I. Mezic, "Nonlinear Koopman modes and a precursor to power system swing instabilities," *Power Systems*, *IEEE Transactions on Power Systems*, vol. 27, no. 3, pp. 1182-1191, 2012.
- [27] Y. Susuki and I. Mezic, "Nonlinear Koopman modes and power system stability assessment without models," *IEEE Transactions on Power Systems*, vol. 29, no. 2, pp. 899-907, 2014.
- [28] B. O. Koopman, "Hamiltonian systems and transformations in Hilbert space," *Proceedings of the National Academy of Sciences of the USA*, vol. 17, no. 5, pp. 315-318, May 1931.
- [29] K. Peterson, "Ergodic Theory," Cambridge: Cambridge University Press, 1983.
- [30] A. Lasota and M. C. Mackey, "Chaos, Fractals, and Noise: Stochastic Aspects of Dynamics," New York: Springer-Verlag, 1994.
- [31] F. Milano, "An open source power system analysis toolbox," *IEEE Transactions on Power Systems*, vol. 20, no. 3, pp. 1199-1206, 2005.